# High-speed focal modulation microscopy using acousto-optical modulators

**Shau Poh Chong[1], Chee Howe Wong[1], Kit Fei Wong[1], Colin J.R. Sheppard[1,2], and Nanguang Chen[1,*]**

[1]*Division of Bioengineering, National University of Singapore, 7 Engineering Drive, Singapore 117576*
[2]*Department of Biological Sciences, National University of Singapore, Singapore 117543*
**biecng@nus.edu.sg*

**Abstract:** Focal Modulation Microscopy (FMM) is a single-photon excitation fluorescence microscopy technique which effectively rejects the out-of-focus fluorescence background that arises when imaging deep inside biological tissues. Here, we report on the implementation of FMM in which laser intensity modulation at the focal plane is achieved using acousto-optic modulators (AOM). The modulation speed is greatly enhanced to the MHz range and thus enables real-time image acquisition. The capability of FMM is demonstrated by imaging fluorescence labeled vasculatures in mouse brain as well as self-made tissue phantom.



**OCIS codes:** (180.2520) Fluorescence microscopy; (110.0113) Imaging through turbid media; (170.0170) Medical optics and biotechnology; (120.4570) Optical design of instruments.

## References and Links

1. J. M. Schmitt, A. Knüttel, and M. Yadlowsky, "Confocal microscopy in turbid media," J. Opt. Soc. Am. A **11**(8), 2226–2235 (1994).
2. P. Theer, and W. Denk, "On the fundamental imaging-depth limit in two-photon microscopy," J. Opt. Soc. Am. A **23**(12), 3139–3149 (2006).
3. J. A. Conchello, and J. W. Lichtman, "Optical sectioning microscopy," Nat. Methods **2**(12), 920–931 (2005).
4. X. Deng, and M. Gu, "Penetration depth of single-, two-, and three-photon fluorescence microscopic imaging through human cortex structures: Monte Carlo simulation," Appl. Opt. **42**(16), 3321–3329 (2003).
5. F. Helmchen, and W. Denk, "Deep tissue two-photon microscopy," Nat. Methods **2**(12), 932–940 (2005).
6. K. Svoboda, and R. Yasuda, "Principles of two-photon excitation microscopy and its applications to neuroscience," Neuron **50**(6), 823–839 (2006).
7. W. Denk, J. H. Strickler, and W. W. Webb, "Two-photon laser scanning fluorescence microscopy," Science **248**(4951), 73–76 (1990).
8. G. H. Patterson, and D. W. Piston, "Photobleaching in two-photon excitation microscopy," Biophys. J. **78**(4), 2159–2162 (2000).
9. H. F. Zhang, K. Maslov, G. Stoica, and L. V. Wang, "Functional photoacoustic microscopy for high-resolution and noninvasive in vivo imaging," Nat. Biotechnol. **24**(7), 848–851 (2006).
10. D. Razansky, M. Distel, C. Vinegoni, R. Ma, N. Perrimon, R. W. Köster, and V. Ntziachristos, "Multispectral opto-acoustic tomography of deep-seated fluorescent proteins in vivo," Nat. Photonics **3**(7), 412–417 (2009).
11. C. Ventalon, R. Heintzmann, and J. Mertz, "Dynamic speckle illumination microscopy with wavelet prefiltering," Opt. Lett. **32**(11), 1417–1419 (2007).
12. M. A. A. Neil, R. Juskaitis, and T. Wilson, "Method of obtaining optical sectioning by using structured light in a conventional microscope," Opt. Lett. **22**(24), 1905–1907 (1997).
13. S. W. Hell, and J. Wichmann, "Breaking the diffraction resolution limit by stimulated emission: stimulated-emission-depletion fluorescence microscopy," Opt. Lett. **19**(11), 780–782 (1994).
14. N. Chen, C. H. Wong, and C. J. Sheppard, "Focal modulation microscopy," Opt. Express **16**(23), 18764–18769 (2008).
15. C. H. Wong, S. P. Chong, C. J. R. Sheppard, and N. Chen, "Simple spatial phase modulator for focal modulation microscopy," Appl. Opt. **48**(17), 3237–3242 (2009).
16. S. P. Chong, C. H. Wong, C. J. R. Sheppard, and N. Chen, "Focal modulation microscopy: a theoretical study," Opt. Lett. **35**(11), 1804–1806 (2010).
17. Y. Li, Y. Song, L. Zhao, G. Gaidosh, A. M. Laties, and R. Wen, "Direct labeling and visualization of blood vessels with lipophilic carbocyanine dye DiL," Nat. Protoc. **3**(11), 1703–1708 (2008).
18. M. Firbank, M. Oda, and D. T. Delpy, "An improved design for a stable and reproducible phantom material for use in near-infrared spectroscopy and imaging," Phys. Med. Biol. **40**(5), 955–961 (1995).
19. W. Mo, and N. Chen, "Fast time-domain diffuse optical tomography using pseudorandom bit sequences," Opt. Express **16**(18), 13643–13650 (2008).

#128993 - $15.00 USD Received 25 May 2010; revised 19 Jul 2010; accepted 23 Sep 2010; published 30 Sep 2010

20. S. J. Lunt, C. Gray, C. C. Reyes-Aldasoro, S. J. Matcher, and G. M. Tozer, "Application of intravital microscopy in studies of tumor microcirculation," J. Biomed. Opt. **15**(1), 011113 (2010).

## 1. Introduction

In recent development of fluorescence microscopy, the extent of out-of-focus fluorescence background is vital in determining the penetration depth achievable in visualization of biological tissues [1,2]. Even conventional Confocal Microscopy (CM) with a detection pinhole to reject out-of-focus fluorescence is limited to use near the tissue surface (tens of microns) as multiple scattering dominates at large depths which could obscure the in-focus details and diminish the appreciable imaging contrast [3]. In multi-photon microscopy (MPM), nonlinear light-matter interaction is being utilized to concentrate the fluorescence excitation in a submicron focal volume that greatly suppressed the out-of-focus excitation and thus could increase the imaging depth up to 1mm [4–7]. However, MPM uses expensive pulse laser. Furthermore, the concern of nonlinear photon-damage/photobleaching [8] and availability of fluorescence probes with large "two-photon absorption cross-section" make single-photon excitation sometimes favored. Another rapidly developed technique termed photo-acoustic tomography (PAT) [9,10] based on ultrasonic detection of pressure waves generated by the absorption of pulse light in elastic media also enable high-resolution visualization of absorbers a few millimeters deep within highly light-scattering living organisms. However, the in-plane spatial resolution of the photo-acoustic images achievable is limited by the effective bandwidth of the ultrasonic detector; leading to few tenths microns diffraction limited spatial resolution and even worse for axial resolution [10]. Dynamic speckle illumination microscopy (DSI) [11] presents a simple yet robust technique to obtain optical sectioning and out-of-focus background rejection with a widefield microscope coupled with speckle illumination and spatial wavelet prefiltering. However, there are no demonstrations of DSI imaging with penetration depth larger than 100um up to date. Structured illumination microscopy (SI) [12] is another widefield microscopy technique that could improve the spatial resolutions up to 2 folds of that of CM by exploiting the interference patterns in the images captured at different angles corresponding to the illumination diffraction gratings. However, SI is limited in acquisition times due to requirement of capturing multiple images, and no penetration depths larger than 100um have been demonstrated as well. Other super-resolution optical imaging techniques such as stimulated emission depletion (STED) microscopy [13] which uses superlocalized depletion of the excited state by stimulated emission with few tens nanometers spatial resolution being demonstrated are severely limited in penetration depth to few tenths microns and limited for deep imaging applications.

Focal Modulation Microscopy [14,15] is an emerging fluorescence microscopy technique that can provide sub-micron spatial resolution at large penetration depths in highly scattering media such as biological tissues by preserving the signal-to-background ratio. In FMM, intensity modulation at focal point is being induced by interference of two periodically phase modulated (or frequency-shifted) excitation beams, which are spatially separated except when brought to the focal point by the objective lens. Ballistic photons contribute mainly to the oscillatory excitation confined exclusively at the focal point as they have well defined phase and polarization compared to scattered photons, though both of them could reach the focal point. The fluorescence emission from the sample is modulated at the same frequency as excitation. Subsequently, by implementing a lock-in technique to demodulate the fluorescence signal collected by the pinhole detector, we can effectively remove fluorescence signal excited by diffusive photons. Experimental [14,15] and theoretical studies [16] of FMM have shown its immense potential in noninvasive imaging of thick biological samples. Previously, we reported our FMM system implemented using tilting plate phase modulator [15] and modulation frequency up to a few kHz has been achieved. However, compared to most commercial laser scanning microscopes with microsecond pixel dwell time, that modulation frequency presents a fundamental limit on the imaging speed, temporal resolution and imaging throughput we can attain. In this letter we would like to describe a novel

#128993 - $15.00 USD Received 25 May 2010; revised 19 Jul 2010; accepted 23 Sep 2010; published 30 Sep 2010

implementation of FMM with AOMs onto a commercial Confocal Microscope and demonstrate the improved image acquisition speed and quality.

## 2. System design

Our FMM system is based on an Olympus FV300 confocal microscope. The main modification on the optical part is a spatial phase modulator (based on AOMs) inserted into the excitation beam path to periodically phase modulates the two excitation beams (see Fig. 1).

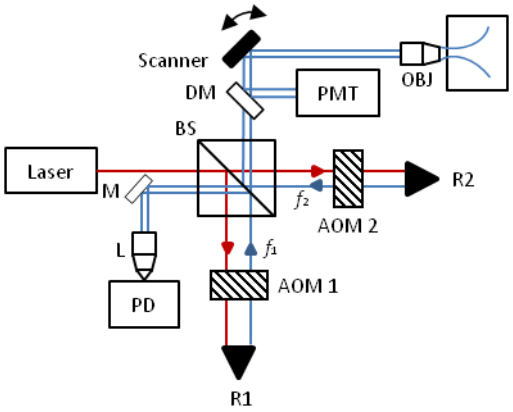


Fig. 1. Setup for a FMM. Laser beam is split by a beam splitter (BS) in which light beam in each arm undergoing frequency shifting by two acoustic-optical modulators (AOM) with different resonance frequencies. Phase-shifted beams are reflected back to the BS by retroreflectors (R1 and R2). They are aligned in parallel non-overlapping manner when being split second times at BS in which one combined beam will be used to generate a reference signal while another combined beam is directed to the scanning unit of Olympus FV300 to excite the samples through the objective lens (OBJ). PD is a photodetector and M is a mirror.

The coherent laser beam is first split by a beam splitter into two beams which then passes through two AOMs (M080-2B/F-GH2) with slightly different resonance frequencies (i.e. $f_1$ and $f_2$) where they undergo zeroth- and first-order diffractions. The first-order diffracted beams which are Doppler shifted at the $f_1$ and $f_2$ on each arm. They are reflected with slight lateral displacement using retroreflectors to return to the same AOMs and then are recombined at beam splitter. It is important to note that the two beams at the moment are Doppler shifted at twice the resonance frequencies of the AOMs respectively as they passed through the AOMs twice. Part of the combined beam is directed towards a fiber-optic photodetector, which generates a reference signal at the optical beating frequency of $2(f_1 - f_2)$. The remaining part of the modulated laser beam is directed to the scanning unit of a conventional CM (Olympus FV300) to excite the biological sample stained with fluorescence probes. The fluorescence emissions are then detected by the built-in PMT detector (Hamamatsu R3896) behind a confocal pinhole. The PMT output is preamplified before feeding to an I/Q demodulator, where the oscillatory component at the beating frequency is picked up by mixing with the reference signal. The demodulated signal is further enhanced by the low-frequency amplifier and is then fed to the data acquisition device of the FV300 system (see Fig. 2 for the signal processing pathway).

#128993 - $15.00 USD Received 25 May 2010; revised 19 Jul 2010; accepted 23 Sep 2010; published 30 Sep 2010

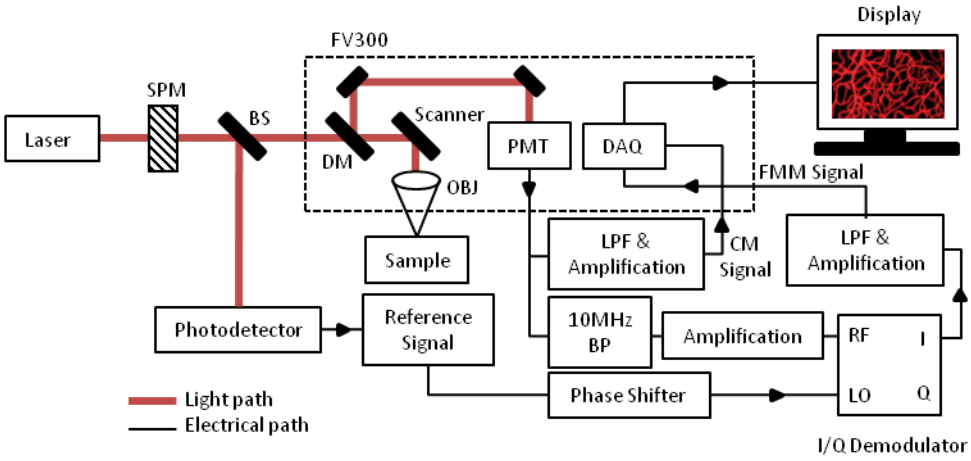


Fig. 2. Flow diagrams showing the signal processing pathway.

The two AOMs we are using have resonant frequencies of 75 MHz and 80 MHz, respectively, resulting in a modulation frequency of 10 MHz. In principle, such a high modulation frequency allows a pixel dwell time as short as 0.1 microseconds. This instrument is a significant improvement in term of imaging speed, stability and noise level compared with the prototype setup we reported previously [14]. CM and FMM images can be captured simultaneously with the same acquisition speed using our current system. The effectiveness of FMM in improving image quality is demonstrated by imaging blood vessels in mouse brain labeled with lipophilic carbocyanine dye DiI ('DiI'; DiIC18(3), Invitrogen) and self-made tissue phantom.

### 3. Sample preparation

The mouse brain samples were prepared using the established techniques described in the literature [17]. A mouse was first sacrificed by overdose with $CO_2$ in a $CO_2$ chamber. A transverse incision was made to open the abdominal cavity. The diaphragm was exposed and cut. The chest was then cut on both sides up to the second rib. The anterior chest wall was turned toward the head of the mouse to expose the chest cavity. The butterfly needle of the perfusion device was inserted into the left ventricle, and the right atrium was punctured. 2ml of standard phosphate buffer solution (PBS) was injected from the perfusion device at the rate of 1-2ml/min for 5min. Then, 5-10ml of the DiI solution was injected at a rate of 1-2ml/min for 5-10 min. Successful perfusion was monitored by observing color change in the ear, nose and palms of the mouse from pale while to purple. Lastly, the fixative (4% paraformaldehyde solution) was injected at a rate of 1-2ml/min for a total of 5min. It should be ensured that there are no air bubbles in the perfusion device as introduction of air into the circulatory system could block blood vessels, resulting in poor perfusion. The stained mouse brain was then extracted, and stored in 4% (wt/vol) paraformaldehyde solution. The whole fixed mouse brain is mounted by mounting medium (Polyvinyl alcohol mounting medium with DABCO®, antifading BioChemika, Sigma-Aldrich) in a coverslip bottom dish with cover (Corning) for imaging using our FMM.

Besides fluorescence imaging, we also apply our FMM system on imaging a cylindrical self-made tissue phantom slab mainly consisted of epoxy-resin, resin hardener, and titanium dioxide ($TiO_2$). The $TiO_2$ powder acts as scattering components and the main contrast agent inside the tissue phantom. This tissue phantom was made based on the procedures reported in literature [18] and is commonly used for calibration in diffuse optical tomography (DOT) [19].

#128993 - $15.00 USD Received 25 May 2010; revised 19 Jul 2010; accepted 23 Sep 2010; published 30 Sep 2010

## 4. Experimental results

The samples were imaged using our FMM system with either objectives UPLSAPO 10x/0.40 numerical aperture (NA) or LUCPLANFLN 20x/0.45 NA to evaluate our FMM system in term of image quality improvement. Here we show the images captured using CM and FMM simultaneously to demonstrate the robustness of FMM in rejecting out-of-focus fluorescence background and retaining high-resolution features even imaging deep inside tissues (depicted by Fig. 3).

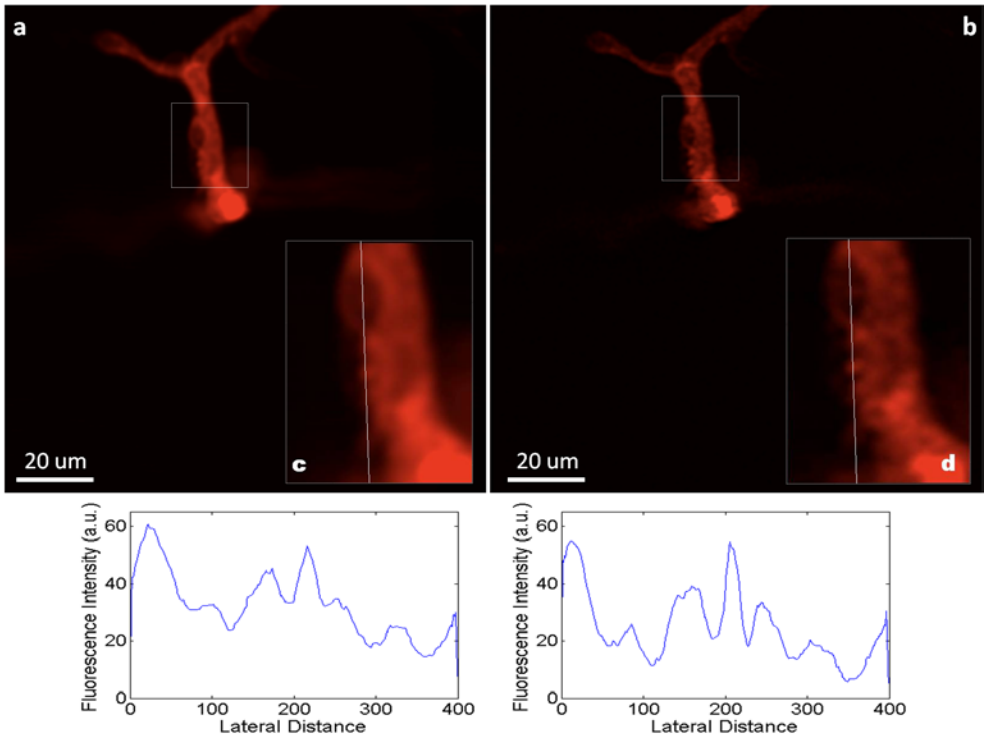


Fig. 3. Demonstration of FMM in retaining high-resolution features by rejecting out-of-focus fluorescence background. A blood vessel bifurcation image acquired with Olympus LUCPLANFLN 20x/0.45 NA using (a) CM and (b) FMM shows much finer features can be revealed by FMM even at penetration depth up 200um. Figure 3 (c) and (d) shows the digital magnification near the bifurcation of the main blood vessel which reveals much richer features on the image captured by FMM. The plot at the bottom of the images shows the intensity profiles of the white lines (top-down) in the images.

A blood vessel bifurcation imaged using CM (Fig. 3 (a)) and FMM (Fig. 3 (b)) shows much finer features can be visualized by FMM clearly at the penetration depth around 200um. Figure 3 (c) and (d) shows the digital magnification near the bifurcation of the main blood vessel (indicated by white boxes in Fig. 3 (a) and (b)) which also reveals better contrast on the fine structures of the blood vessels by the image captured by FMM as compared to CM. From the intensity profiles spanning the both white lines (top-down) in the Fig. 3 (c) and (d), we can also observe that the peaks are more clearly visible and distinctive from each others in the FMM image, with significant reduction in background as well. This indicates that our FMM system can provide better image contrast and more structural information of the tissue being studied. All the images were taken at 512x512 pixels, with a pixel dwell times of around 10 us, resulting image acquisition time of around 2.7s.

We performed imaging in the tissue phantom over the depths of 300-400um with 0.5um increments. The full results for the stack of images captured can be seen in a movie online at the supplementary material. A single frame from the movie shows the image of a cluster of

#128993 - $15.00 USD Received 25 May 2010; revised 19 Jul 2010; accepted 23 Sep 2010; published 30 Sep 2010

$TiO_2$ powder (see Fig. 4) embedded at 320um inside the self-made tissue phantom using CM and FMM operating in reflectance mode to detect the back-reflected light.

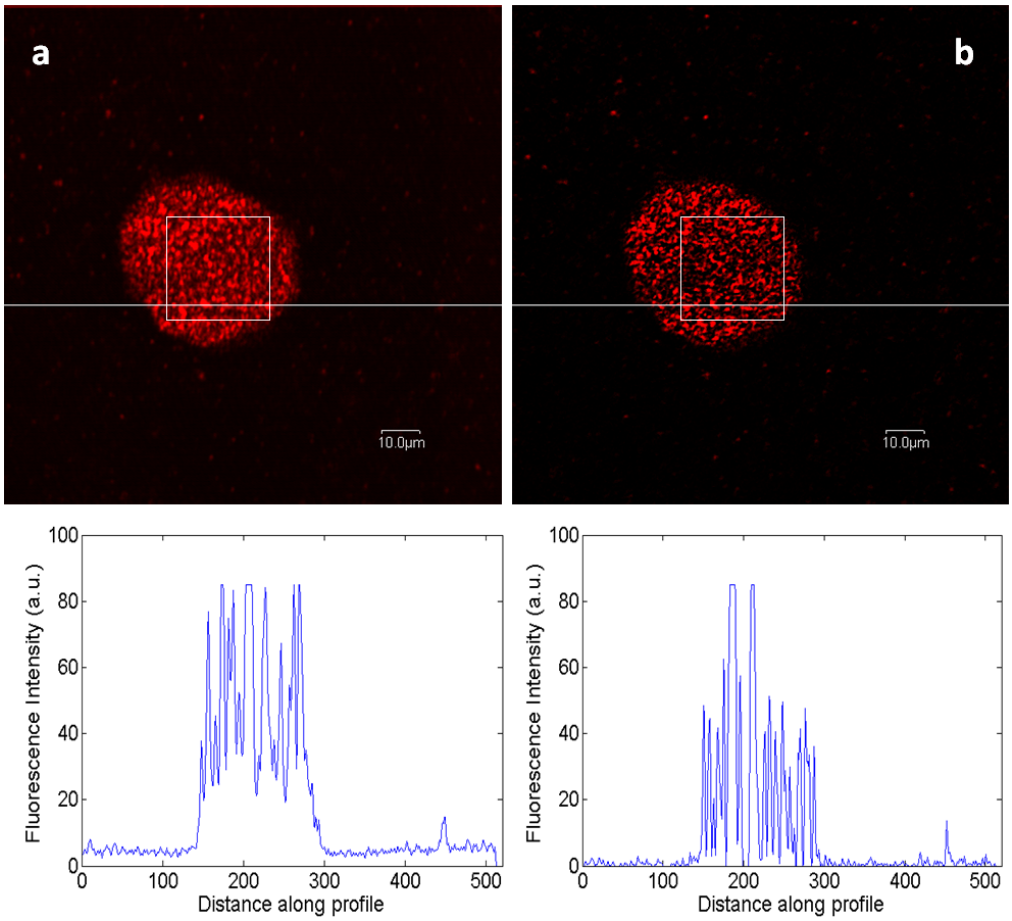


Fig. 4. (Media 1) Image of cluster of $TiO_2$ embedded 320um inside tissue phantom captured with Olympus LUCPLANFLN 20x/0.45 NA using (a) CM and (b) FMM. Better image quality is achieved using FMM, with less blurring and structures are more clearly distinguishable due to sharp boundaries. The plot at the bottom of the images shows the intensity profile of the white lines in the images. Peaks are more distinct with better contrast can be observed.

Again, FMM (see Fig. 4 (b)) significantly improve the image quality by providing better contrast and sharp edges compared to CM with blurring mainly caused by multiple scattering effects. The peaks are also more clearly distinguished from each other in FMM shown by the intensity profile spanning the white line (left-right), with higher signal-to-background ratio due to lower background intensity. All the images were taken at 512x512 pixels, with a pixel dwell times of around 10 us, resulting image acquisition time of around 2.7s. To perform more quantitative analysis of image quality improvement by FMM, we selected a pair of identical region of interest (ROI) from Fig. 4 (a) and (b) respectively and compare their normalized spectra (with respect to the dc values). From Fig. 5, we can see that the high frequency components (>1 cycle/μm) in the FMM image are about 13 dB stronger than those in the CM image. This can be translated to a 13 dB improvement in the signal to background ratio provided by FMM. Our theoretical model [16] predicted a 20 dB enhancement by FMM at a similar imaging depth of 2 scattering mean free paths (the scattering coefficient of our tissue phantom is around 6 $cm^{-1}$ [19]). The discrepancy is probably due to slight overlapping

#128993 - $15.00 USD Received 25 May 2010; revised 19 Jul 2010; accepted 23 Sep 2010; published 30 Sep 2010

of the two excitation beams and the resultant residual intensity modulation which can be minimized by improved modulator designs.

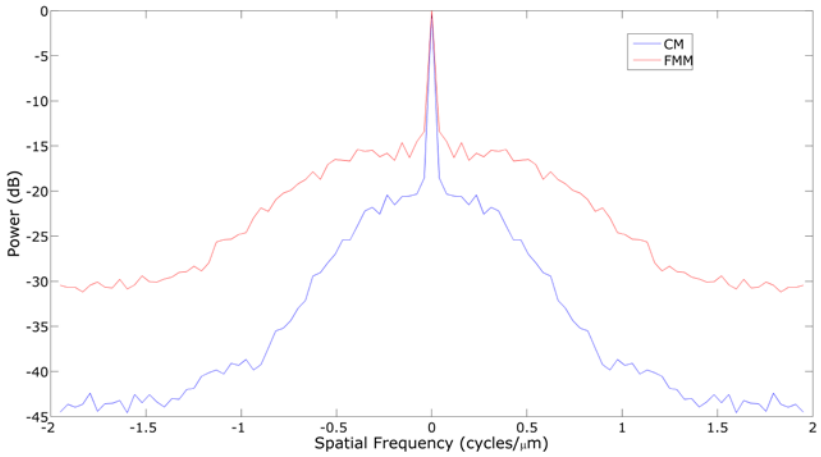


Fig. 5. Normalized spatial spectra (with respect to dc values) of the region of interests labeled by square boxes in Fig. 4 (a) and (b) showing the spatial frequency components of CM and FMM respectively.

## 5. Discussion and conclusion

We have validated the capability of FMM in improving image quality at large penetration depth by visualizing blood vessels in whole mouse brain as well as tissue phantom. We emphasized that as the mouse brain samples are specifically stained in which only blood vessels void of blood (one of the major absorbers and scatterers inside biological tissues) are labeled with DiI, generally less background will be observed while larger penetration depth is expected compared to uniformly stained samples. Nevertheless, FMM can work robustly in detecting fluorescence by ballistic photons and rejecting out-of-focus fluorescence background even at the large depth. This is an important feature for investigations and characterizations of thick tissue with sub-micron spatial resolution when confocal pinhole fails to reject majority of the out-of-focus fluorescence background. In this paper, better characterization of microvasculatures in animal model over large observation volume using FMM can be potentially useful especially for quantification of angiogenesis in term of density/diameter of blood vessels in live animal cancer model [20]. We also highlight that though FMM can reject most of the background, it cannot increase the signal level and thus if the FMM signal falls below the shot noise floor at extreme depths, other strategies (i.e. denoise image processing and/or extended image acquisition time) may be needed to improve the image quality.

A modulation frequency of 160 MHz can be achieved if only a single AOM is used. However, a too high modulation frequency could cause significant attenuation of the FMM signals as the signal intensity is proportional to $\exp(-2\pi f\tau)$ in which f is the modulation frequencies and $\tau$ is the lifetime of fluorescent probes. As most of the fluorescent molecules have a typical lifetime of a few nanoseconds, deterioration of the signal-to-noise ratio will thus be a serious problem at large penetration depths. The 10 MHz we choose falls in the optimal frequency range for fast image acquisition and negligible signal attenuation, and it is compatible with available demodulation components. It should be noticed also FMM can extend the penetration depths for imaging in fluorescence and reflectance mode, while MPM is only compatible to fluorescence imaging. In future, the issues of inherent Poisson statistical noise that gradually becoming significant in the case of low intensity signal related to deep

#128993 - $15.00 USD Received 25 May 2010; revised 19 Jul 2010; accepted 23 Sep 2010; published 30 Sep 2010

imaging of biological tissues and further improvement of the image quality with the inclusion of Poisson noise removal will be studied.

To conclude, we have developed and experimentally demonstrated FMM implemented with AOMs to provide fluorescence visualization of fixed biological samples with large penetration depths. Compared with our previous setup, the imaging speed for the FMM implemented with AOM has been significantly improved and thus showing promising potential in real-time in vivo imaging of thick biological tissues. Further improvements are still underway, especially in minimizing optical and electronic noise in FMM which could further extend its penetration depth, enriching its applications in biological research and clinical diagnoses such as adaptation to fluorescence lifetime imaging.

**Acknowledgments**

This work is partially supported by the research grant from Bioimaging Consortium/Singapore Stem Cell Consortium, A*STAR (SBIC-SSCC RP C-003/2007). We thank Dr Scott Lee Trasti and Justin David Patch from Veterinary Diagnostic Laboratory of National University of Singapore for their guidance in performing perfusion and extraction of mouse brain samples.

#128993 - $15.00 USD Received 25 May 2010; revised 19 Jul 2010; accepted 23 Sep 2010; published 30 Sep 2010